

Theoretical investigation of interaction energies between carbon and BN nanotubes with human hepcidin peptides: insights into the semi empirical and Monte Carlo methods

Reza Rasoolzadeh¹, Faramarz Mehrnejad^{2*}, Majid Taghdir³, Parichehreh Yaghmaei¹

¹Department of Biology, Science and Research Branch, Islamic Azad University, Tehran, Iran

²Department of Life Sciences Engineering, Faculty of New Sciences & Technologies, University of Tehran, Tehran, Iran

³Department of Biophysics, Faculty of Biological Sciences, Tarbiat Modares University, Tehran, Iran

*corresponding author e-mail address: Mehrnejad@ut.ac.ir

ABSTRACT

Interactions of Human Hepcidin peptides with carbon and boron nitride nanotubes can perform superior properties in a wide range of biological and chemical applications. In the present paper, we investigate some computational studies about this subject by using of Semi-Empirical and Monte Carlo methods both methods structural and mechanical differences between them in gas phase alone and when covalently linked to nanotubes. A substantial conformational change of the Hepcidin-20 and Hepcidin-25 peptides domain can not completely create by the interaction between nanotubes and the peptides. These are due to the presence of distorted β -sheet structure and multiple disulfide bonds. The difference in the calculated values for both peptides is due to be differences in both their N-terminal, and loops. Measurements of potential energy of human hepcidin peptides in different nanotubes and in two different temperatures revealed that at time step 0 to 5 ns, our system has a maximum energy level, and at time step size 40 to 50 ns, has the minimum energy level and maximum stability.

Keywords: nanotubes, human hepcidin peptides, semi empirical, Monte Carlo.

1. INTRODUCTION

Human hepcidin (hepatic bactericidal protein) is a small 25 amino acid amphipathic peptide hormone first found in human blood ultrafiltrate and urine samples [1, 2]. It is a cysteine-rich cationic antimicrobial peptide with antibacterial and antifungal activity. More human hepcidin is produced primarily in hepatocytes, while synthesis of hepcidin is recently identified in other tissues and cells (bacteria-activated neutrophils and macrophages) although to a much smaller extent than the hepatocytes [3, 4]. A precursor of hepcidin – preprohepcidin is synthesized by the human liver which is 84 amino acids protein. The first 24 amino acids of preprohepcidin at N-terminal signal peptide is subsequently cleaved to produce prohepcidin. Pro-hepcidin is then cleaved to generate the bioactive 25 amino acid peptides that are differentiable in both blood and urine. In addition to the 25 amino acid form as the predominant form, two peptides shorter at the amino terminus were also found in human urine, hepcidin-22 and hepcidin-20 [5]. There are two predominant forms which act as the principal regulator of iron with 25 and 20 residues, contain a distorted β -sheet shape with a hairpin loop and are connected by disulfide pairing of Cys residues and hydrogen bonds between the two antiparallel strands [6,7]. Human hepcidin plays a key role in iron absorption and iron delivery by directly binding the membrane iron exporter, ferroportin, which causes its internalization and degradation, decreasing iron export from the cell and reducing serum iron availability [8, 9]

Carbon nanotubes (CNTs) are the most common type of carbon nanoparticles which have attracted important attention due to the variety of their unique structural properties such as of nano-size, high aspect ratio, strong mechanical strength, electric conductivity, optical, thermal stability [10] and high surface area in many scientific fields, including biomedical sciences [11],

biosensors [12], drug carrier [13], other hybrid materials [14]. Additionally, they are noncytotoxic [15]. Structurally, carbon nanotubes could serve into single-walled carbon nanotubes (SWNTs), and multiple-walled carbon nanotubes (MWNTs) [16]. They can also be classified into zigzag, armchair, and helix forms. Many studies have been performed to investigate non-carbon based inorganic nanotubes because of their unique chemical inertness, and structural stability properties.

Among them, boron nitride nanotubes (BNNTs) have been viewed as proper materials with the unique properties similar to the CNTs, therefore they are an appropriate candidate for medical applications such as drug delivery [11]. In contrast to the CNTs, which behave as metal or semiconductor depending on their tubular diameter and chirality, the BNNTs are all semiconductors with almost the same band gaps of 5.5 eV independent of the restricting factors [17]. In addition, the polarity and ionicity of the nanotubes are increased due to the slight positive charge of the boron and slight negative charge of the nitride atom. The particular nature of BNNTs is dependent on the nature of their partial ionic bonds. Experimenting BNNTs on human cells indicated that these nanotubes are nontoxic to health and environment due to their chemical inertness, structural stability and corroborate that BNNTs are more appropriate for biomedical applications [18].

A numerous number of research papers can be attributed to the interaction of peptides and proteins on CNT surfaces with the help of experimental methods [19], while only a few types of researches exist about the mechanism of interactions between peptides and SWCNTs. Salvador-Morales et al. have shown that susceptibility of lung infection and emphysema in mice created by CNT binding with pulmonary surfactant proteins A and D [20].

WW domains (i.e. YAP65, YJQ8, and PIN1) took by Ruhong Zhou and co-workers to investigate the interaction of CNT with protein and the subsequent impact on the protein activity [21]. However, the understanding of the interactions details the peptide and the SWNT is necessary for these bio-applications of CNTs, because of these interactions can increase their biocompatibility [22] or affected the toxicity and non-toxic properties of nanotubes [23]. In general, the interactions between peptides and CNTs can be addressed by either covalent conjugation or noncovalent absorption [24]. Noncovalent is consist of van der Waals interactions, π - π interactions, and hydrophobic interactions, while covalent is consist of functionalization of CNTs with COOH groups and enhancing their solubility in water [25, 26]. Furthermore, BNNT has a good interaction with proteins. Chen has affirmed that BNNTs interacted with proteins and thus these nanotubes can be utilized in biocompatible materials [27]. The exact details of CNTs interactions with peptides are not obvious due to the lack of experimental methods. However, calculations of free energy differences can investigate using computational chemistry methods of semi-empirical and Monte Carlo (MC) for accurately studying the details of molecular interactions in complex systems at the atomic level. Cheng et al. performed Monte Carlo simulation method and 2D hydrophobic-polar lattice

model are used by Cheng et al. to investigate interactions between model peptides and CNTs [28]. Therefore, it is remarkable to simulate the interaction between peptides and CNTs using Monte Carlo simulation and scrutinize the molecular mechanism of the interaction.

To the best of our knowledge, no experimental and theoretical studies about the mechanism of interactions between the human hepcidin peptides and the carbon and boron nitride nanotubes have not been previously reported. Therefore, a great deal of our own work is to investigate the behavior of Hepcidin-20 and Hepcidin- 25 in body and room temperatures, as well as the interaction human hepcidin peptides with carbon and boron nitride nanotubes. As a result, to this time, a comparative study on the electronic structure properties of BNNT and CNT and their effects on peptides structure and function using quantum chemistry method as an effective method of studying biomolecules has been reported. Calculations of energy differences obtained using methods of Semi-Empirical and Monte Carlo will give us valuable information about nanotubes interactions. Computer simulations with these methods can cause to a better understanding of the thermodynamic and kinetic parameters of such peptides and create better insight into design, production, and structural changes of peptides in various processes

2. EXPERIMENTAL SECTION

2.1. Computational details. In the current study, we considered the behavior of Hepcidin-20 and Hepcidin- 25 on three representative models of the zigzag multi-wall carbon, zigzag single wall (6, 6) carbon and boron nitride nanotubes that were covalently added to them with lengths of 14 Å. The multi-wall carbon and (6, 6) carbon and BN nanotubes displayed in Fig. 1. The PDB files of both systems were taken from protein data bank (PDB code 1M4E for Hepcidin-20 and PDB code 1M4F for Hepcidin-25). The first structure is the (6, 6) SWCNT that was made of 144 C atoms forming 12 layers of atoms along the tube axis (Fig. 1c). The second structure is the (6, 6) SWBNNT that has been created of 72 N and 72 B atoms which could be broken up into six layers of B and six layers of N atoms (see Fig. 1d). In both of the models, the ends of the nanotube are saturated by 24-hydrogen atoms in order to elude dangling bonds and reducing calculation time. The third structure is the MWCNT with 215 atoms carbons forming 12 layer atoms along the tube axis, also the ends of the nanotube are saturated by 36 hydrogen atoms (Fig.1e). The optimized geometries and the properties of the electronic and structural properties of the (6, 6) pristine and peptides attached to pristine were calculated by means Gaussian 03 program with the Hartree-Fock (HF) methods at STO-3G, 6-31G basis sets of the theory [29, 30].

2.2. Semi-Empirical Method. The semi-empirical molecular orbital methods, their setup is obtained from Hartree-Fock theory, the design of proximate energy expressions and the experimental parameters are utilized to attain higher accuracy than the underlying ab initio theory. Their computational output causes them appropriate for the investigation of biochemical systems and

solid materials [31]. The Austin Model 1 (AM1) and Parameterized Model number 3 (PM3) semi-empirical methods within the Restricted Hartree-Fock (RHF) formalism are appropriate to investigate carbon systems [32]. The semi-empirical calculations optimize all atomic positions and lattice parameters with minimizing total energy and atomic forces. These calculations performed with optimizing parameters such as total energy, binding energy, isolated atomic energy, electronic energy, core-core interaction and heat of formation for Hepcidin-20 and Hepcidin- 25 before and after their interaction with the nanotubes in which the best relation have been obtained. All semi-empirical calculations presented here were performed with AM1and PM3 methods.

2.3. Molecular Mechanics and Quantum Mechanics (Monte Carlo Simulation). Monte Carlo simulation is a computerized mathematical technique to mean entirely different things. All Monte Carlo methods are useful for obtaining numerical solutions to problems, which are too complicated to solve analytically. Molecular thermodynamic properties, as well as minimum energy structures, can be determined from the Monte Carlo methods (33). This method is one of the most commonly used numerical techniques in the fields of statistical physics, field theory, quantum mechanics, and others [34]. In the Monte Carlo method, the precision of the algorithm is specified by random displacement, as well as, differences in force field are demonstrated by comparing the calculated energy using OPLS force field.

In this research, the quantum and molecular mechanics chemical study was performed using Monte Carlo simulation. We scrutinize the temperature effects (300 and 310 K) for calculation

of peptides before and after their interaction with nanotubes with OPLS in various molecular mechanics (MM) methods. The temperatures 300 and 310 K has selected because are close to the normal temperature of the human body. Selecting a force field that is well performed for the molecular system under study is very significant. The calculations were carried out using the

3. RESULTS SECTION

The main objective of this section is to analyze both structural and mechanical differences between Hepcidin-20 and Hepcidin-25 (Figure 1a) and their interaction with SWCNT, MWCNT, and BNNT. In the gas phase, our system was simulated using Monte Carlo and Semi-Empirical with a time step of 50 ns and without any constraints. The study of energies was kept at two different temperatures 300 and 310 K.

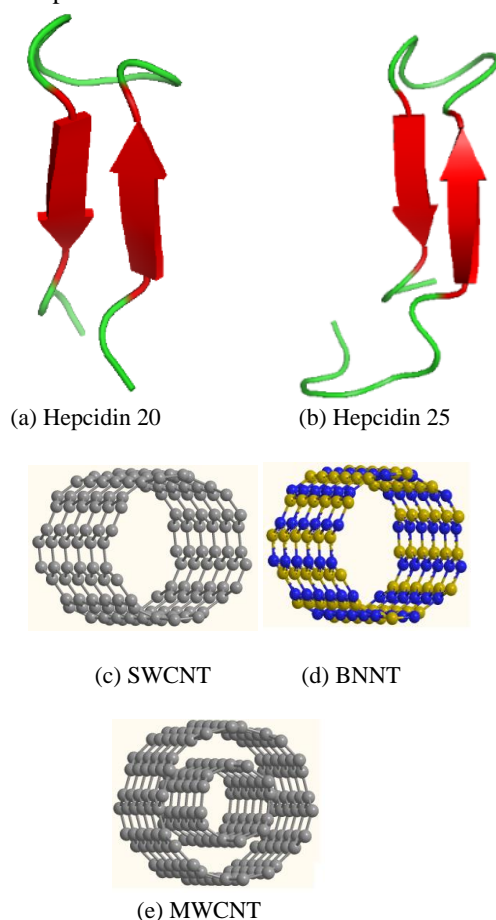


Figure 1. Schematic illustration of Hepcidin-20 and Hepcidin-25 and nanotubes.

The Energy parameters such as total, potential and kinetic energy were calculated by the Monte Carlo Simulation. As it is clear from Table 1, the maximum amounts of the peptides in both different temperatures were related to Hep20+MWCNT. Since the potential energy amounts and total are also dependent on the kinetic energy, but the remarkable point is that the amount kinetic energy in the Hep20+BNNT complex is more than Hep20+SWCNT complex. However, the amount of potential energy is reversed that this point affected in the total energy and the amount of total energy Hep20+SWCNT is more than Hep20+BNNT. To exhibit the comparison of four complexes in OPLS force field, optimized

HyperChem professional release 7.01 package of the program [35]. As a result, we calculated total energy (E_{tot}), the potential (E_{pot}) and kinetic (E_{kin}) energy (kcal/mol) in two different temperatures (300–310) and time of simulations is 50 ns.

energy parameters of the systems during simulation were obtained and listed in Table 1 [36].

As shown in figure 2, the changes process of the potential energy for the four systems have a descending trend and follows the constant process that can see in the figure. It is worth noting that in the Hep20+SWCNT system, the amount of the potential energy changes from the initial state and the final state in 300 K is more than 310 K. The Hep20+MWCNT complex had more negative ΔE in 300 K than that of 310 K, whereas for Hep20+BNNT complex, this ratio is reversed. Interestingly, the Hep20+BNNT complex has approximately the amount of equal ΔE in both temperatures. [37].

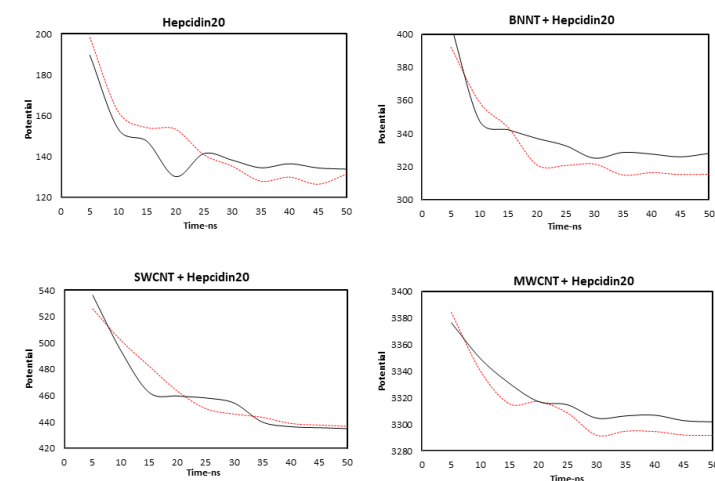


Figure 2. The potential energy diagram(kcal/mol) versus simulation time (ns) during Monte Carlo (MC) simulation at 300K (---) and 310K (—).

In the study of molecular mechanics (Monte Carlo) for hepcidin25 and its complex with MWCNT, BNNT, and SWCNT, we realized that ΔE values in different conditions and both temperatures 300°K and 310°K are less than hepcidin 20. ΔE changes in the hepcidin25 are less due to the structure of this peptide. The difference between the peptides is due to the N-terminal and loop that is placed in the middle of the protein. The N-terminal in the hepcidin20 is included ILE, Cys, and ILE amino acids while in hepcidin25 is included the Asp, Thr, His and Phe amino acids that the energy changes in hepcidin25 are due to the steric hindrance of aromatic ring in His and Phe, which can be caused more stable for the hepcidin25 peptide. In order to investigate the potential energy comparison of four complexes in the OPLS force field during the simulation, the optimized energy parameters were calculated and listed in Table 2 [38,39].

The evolution of the potential energy of the hepcidin25, Hep25+SWCNT, Hep25+MWCNT, and Hep25+BNNT is presented in Fig. 3. The comparison between diagrams shows that

the potential energy changes of the both hepcidin25 and Hep25+BNNT have been reached to in the about simulation time of 25ns, whereas this relative stability accrues for Hep25+SWCNT and Hep25+MWCNT at about 35 ns.

The comparison between Fig. 2 and 3 (Table 2 and 3) demonstrates that the ΔE value in the Hep20 complexes is more negative than that of the Hep25 complexes. This evidence shows more stability Hep25 complexes. In order to investigate the characterization of total energy, binding energy, isolated atomic energy, electronic energy, core–core interaction and heat of formation for the four systems named, the Semi-Empirical simulation was performed. In this study, PM3 and AM1 methods are used, which can be observed in Table 3. The changes process of these energies is very noticeable with respect to the type nanoparticles atoms and their number. The results of the calculations demonstrated that binding energy of the Hep20 is lower in AM1 and the total energies of these compounds in the gas phase were in the order, $E(\text{MWCNT}) > E(\text{BNNT}) > E(\text{SWCNT})$. This order for total energy is like before.

On the other hand, the changes trend of the total energy and binding energy is equal to the PM3 method. The core–core interaction parameter in the Hep20 is in the order, $\text{MWCNT} > \text{BNNT} > \text{SWCNT} > \text{Hep20}$ [32, 40].

By comparison of Semi-Empirical calculations for the Hep20 and Hep25 complexes, we found that the calculated energy values in the PM3 method are less than in AM1. The PM3 method investigates phosphorus existing in peptides for better and adjusts energy values that are due to the less investigation of steric hindrance and less effect of non-bonding. We can observe these results in table 4 [35].

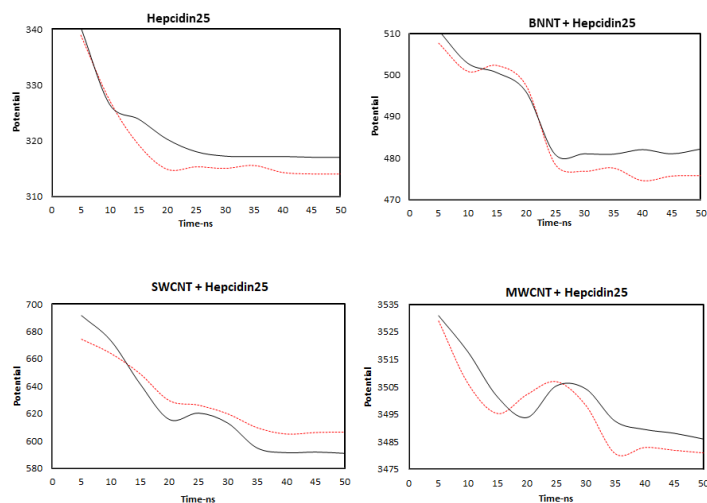


Figure 3. The potential energy diagram (kcal/mol) versus simulation time (ns) during Monte Carlo (MC) simulation at 300K (-----) and 310K (—).

The changes process of the binding energy for complexes of Hepcidin20 has better evolution in PM3 rather than AM1. By comparison of the semi-empirical calculation for hepcidin25,

Hep25+SWCNT, Hep25+MWCNT and Hep25+BNNT in Figure 4, we have found the best relation coefficients of $R^2 = 0.838$ (Electronic Energy), $R^2 = 0.876$ (Core–Core Interaction), $R^2 = 0.917$ (bonding energy) and $R^2 = 0.917$ (Heat of Formation) for PM3. In addition, we observed this trend for Hepcidin25 with the desired results in Figure 5. We have achieved. The best relation coefficients of $R^2 = 0.974$ (Electronic Energy), $R^2 = 0.990$ (Core–Core Interaction), $R^2 = 0.939$ (bonding energy) and $R^2 = 0.908$ (Heat of Formation) for PM3. [41].

By comparison of the Semi-Empirical calculations between Fig. 4 and 5 (Table 3 and 4), we gain this result that deviations trend for Hepcidin20 is more than Hepcidin25 which is related to structural stability and less effect of nanoparticles on Hepcidin25 [42].

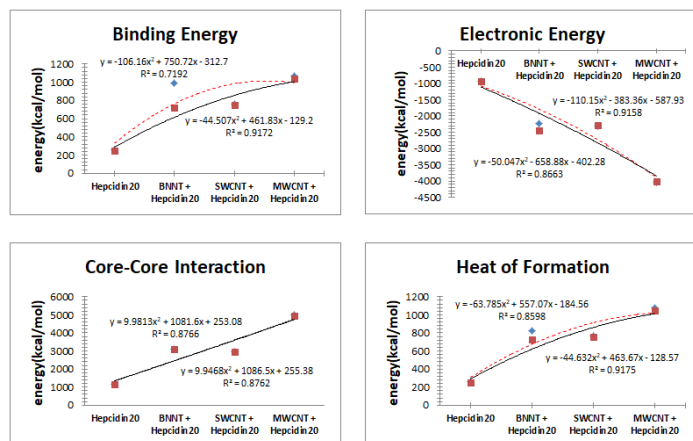


Figure 4. Optimized parameters of binding energy, electronic energy, core–core interaction and heat of formation(Kcal/mol) for Hepcidin20 , BNNT + Hepcidin20 , SWCNT + Hepcidin20 and MWCNT+Hepcidin20 in gas phase by AM1 (-----)and PM3 (—) calculation.

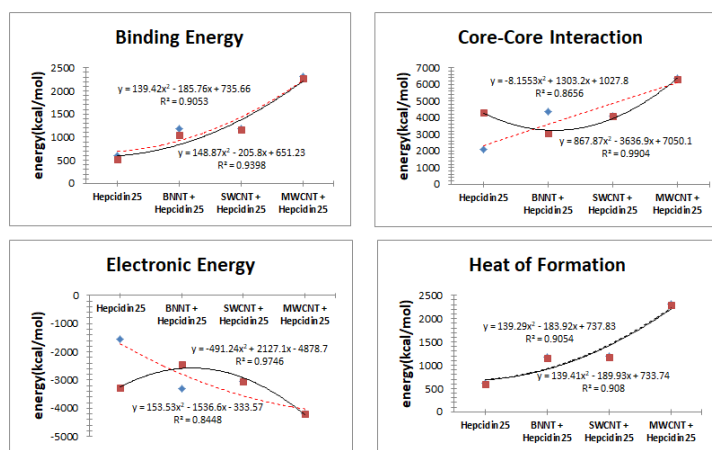


Figure 5. Optimized parameters of binding energy, electronic energy, core–core interaction and heat of formation(Kcal/mol) for Hepcidin25 BNNT + Hepcidin25 , SWCNT + Hepcidin25 and MWCNT + Hepcidin25 in gas phase by AM1 (-----) and PM3 (—) calculation.

Theoretical investigation of interaction energies between carbon and BN nanotubes with human hepcidin peptides: insights into the semi empirical and Monte Carlo methods

Table 1. Calculated optimized energy parameter(kcal/mol) of Hepcidin20, BNNT + Hepcidin20, SWCNT + Hepcidin20 and MWCNT + Hepcidin20 in OPLS force field by molecular mechanics method (monte Carlo).

<i>T</i> (K)	<i>Time step ns</i>	<i>Hepcidin20 (kcal/mol)</i>			<i>BNNT + Hepcidin20 (kcal/mol)</i>			<i>MWCNT + Hepcidin20 (kcal/mol)</i>			<i>SWCNT + Hepcidin20 (kcal/mol)</i>		
		Kinetic energy	Potential energy	Total energy	Kinetic energy	Potential energy	Total energy	Kinetic energy	Potential energy	Total energy	Kinetic energy	Potential energy	Total energy
300	5	177.953	198.3362	376.2892	328.1847	392.2737	720.4584	403.3006	3384.098	3787.398	306.723	525.9492	832.6722
	10		161.9143	339.8673		358.9076	687.0923		3340.193	3743.494		502.0129	808.7359
	15		154.2366	332.1896		343.615	671.7997		3315.479	3718.779		482.3741	789.0971
	20		153.5123	331.4653		321.1693	649.354		3317.132	3720.432		463.4661	770.1891
	25		140.9865	318.9395		320.8299	649.0146		3308.637	3711.937		450.1908	756.9138
	30		135.3709	313.3239		321.7487	649.9334		3291.848	3695.149		446.0465	752.7695
	35		128.0945	306.0475		315.1203	643.305		3294.954	3709.338		443.6051	750.3281
	40		130.0872	308.0402		316.5124	644.6971		3294.73	3698.031		438.9106	745.6336
	45		126.6073	304.5603		315.379	643.5637		3292.048	3685.622		437.7753	744.4983
	50		131.6297	309.5827		315.5498	643.7345		3291.901	3675.848		436.8109	743.5339
310	5	183.8848	189.6997	373.5845	339.1242	405.6231	744.7473	416.7439	3376.384	3793.128	316.9471	536.2773	853.2244
	10		153.4963	337.3811		347.6578	686.782		3349.457	3766.201		494.1914	811.1385
	15		147.5824	331.4672		342.3723	681.4965		3330.794	3747.538		462.4127	779.3598
	20		130.3065	314.1913		337.1288	676.253		3317.115	3733.859		459.7508	776.6979
	25		141.5532	325.438		332.756	671.8802		3314.71	3731.454		458.2525	775.1996
	30		138.3387	322.2235		325.2242	664.3484		3304.713	3721.457		454.4444	771.3915
	35		134.6345	318.5193		328.7286	667.8528		3306.394	3723.138		440.0015	756.9486
	40		136.5731	320.4579		327.6987	666.8229		3306.94	3723.684		436.4625	753.4096
	45		134.534	318.4188		326.0401	665.1643		3302.812	3719.556		435.6988	752.6459
	50		133.973	317.8578		328.1025	667.2267		3301.914	3718.658		435.0187	751.9658

Table 2. Calculated optimized energy parameter (kcal/mol) of Hepcidin25, BNNT + Hepcidin25, SWCNT + Hepcidin25 and MWCNT + Hepcidin25 in OPLS force field by molecular mechanics method (Monte Carlo).

<i>T</i> (K)	<i>Time step ns</i>	<i>Hepcidin25 (kcal/mol)</i>			<i>BNNT + Hepcidin25 (kcal/mol)</i>			<i>MWCNT + Hepcidin25 (kcal/mol)</i>			<i>SWCNT + Hepcidin25 (kcal/mol)</i>		
		Kinetic energy	Potential energy	Total energy	Kinetic energy	Potential energy	Total energy	Kinetic energy	Potential energy	Total energy	Kinetic energy	Potential energy	Total energy
300	5	375.5792	338.951	714.5302	525.8109	507.6487	1033.46	600.926	3528.9826	4129.909	504.3492	674.4566	1178.806
	10		327.229	702.8082		500.8485	1026.659		3506.158	4107.084		664.0859	1168.435
	15		319.2777	694.8569		502.2802	1028.091		3495.294	4096.22		649.2126	1153.562
	20		314.834	690.4132		497.5091	1023.32		3502.204	4103.13		629.4828	1133.832
	25		315.2943	690.8735		478.5206	1004.332		3506.901	4107.827		626.2118	1130.561
	30		315.0077	690.5869		476.8119	1002.623		3498.243	4099.169		619.8222	1124.171
	35		315.5422	691.1214		477.6019	1003.413		3480.6748	4081.601		609.728	1114.077
	40		314.2804	689.8596		474.5454	1000.356		3482.941	4083.867		605.0489	1109.398
	45		314.0157	689.5949		475.6428	1001.454		3481.9287	4082.855		606.1848	1110.534
	50		313.9872	689.5664		475.7319	1001.543		3480.9487	4081.875		606.5334	1110.883
310	5	388.0985	340.3704	728.4689	543.3379	510.6971	1054.035	620.9577	3530.898	4151.856	521.1609	691.7341	1212.895
	10		326.5013	714.5998		502.8065	1046.144		3517.678	4138.636		673.4812	1194.642
	15		323.8788	711.9773		500.5438	1043.882		3501.3214	4122.279		641.855	1163.016
	20		320.2281	708.3266		495.9598	1039.298		3493.8271	4114.785		615.715	1136.876
	25		318.0082	706.1067		480.8781	1024.216		3505.3557	4126.313		620.3791	1141.54
	30		317.2121	705.3106		481.0017	1024.34		3504.252	4125.21		613.0535	1134.214
	35		317.1288	705.2273		480.9105	1024.248		3492.484	4113.442		594.8715	1116.032
	40		317.1499	705.2484		482.0016	1025.34		3489.4809	4110.439		591.3907	1112.552
	45		317.0078	705.1063		481.0008	1024.339		3488.1007	4109.058		591.8743	1113.035
	50		316.9987	705.0972		482.149	1025.487		3486.0029	4106.961		590.8813	1112.042

Theoretical investigation of interaction energies between carbon and BN nanotubes with human hepcidin peptides: insights into the semi empirical and Monte Carlo methods

Table 3. Optimized parameters of total energy, binding energy, isolated atomic energy, electronic energy, core–core interaction, and heat of formation (Kcal/mol) for Hepcidin20, BNNT + Hepcidin20, SWCNT + Hepcidin20 and MWCNT + Hepcidin20 by AM1 and PM3 calculations.

Methods	AM1				PM3			
Energy(kCal/mol)	<i>Hepcidin20</i>	<i>BNNT + Hepcidin20</i>	<i>MWCNT + Hepcidin20</i>	<i>SWCNT + Hepcidin20</i>	<i>Hepcidin20</i>	<i>BNNT + Hepcidin20</i>	<i>MWCNT + Hepcidin20</i>	<i>SWCNT + Hepcidin20</i>
<i>Total Energy</i>	199.25610	886.02261	947.56471	661.62926	199.89716	636.60992	934.14986	657.70032
<i>Binding Energy</i>	257.02931	988.61372	1066.46458	759.52285	251.68946	725.72279	1042.43309	746.42970
<i>Isolated Atomic Energy</i>	-57.77320	-102.59111	-118.89986	-97.89358	-51.79229	-89.11287	-108.28323	-88.72937
<i>Electronic Energy</i>	-939.01298	-2222.56947	-4026.28264	-2302.10772	-932.44998	-2456.50877	-4017.31381	-2293.06678
<i>Core-Core Interaction</i>	1138.26909	3108.59208	4973.84736	2963.73698	1132.34715	3093.11870	4951.46367	2950.76711
<i>Heat of Formation</i>	259.26953	992.76963	1072.58360	764.22389	253.92969	729.87870	1048.55211	751.13075

Table 4. Optimized parameters of total energy, binding energy, isolated atomic energy, electronic energy, core–core interaction and heat of formation(Kcal/mol) for Hepcidin25, BNNT + Hepcidin25, SWCNT + Hepcidin25 and MWCNT + Hepcidin25 by AM1 and PM3 calculations.

Methods	AM1				PM3			
Energy(kCal/mol)	<i>Hepcidin25</i>	<i>BNNT + Hepcidin25</i>	<i>MWCNT + Hepcidin25</i>	<i>SWCNT + Hepcidin25</i>	<i>Hepcidin25</i>	<i>BNNT + Hepcidin25</i>	<i>MWCNT + Hepcidin25</i>	<i>SWCNT + Hepcidin25</i>
<i>Total Energy</i>	524.84475	1053.00688	2167.95197	1058.30580	524.09390	1045.66403	2151.34122	1053.86196
<i>Binding Energy</i>	604.19611	1177.17615	2308.430	1177.77754	596.31701	1155.20772	2280.05528	1163.02216
<i>Isolated Atomic Energy</i>	-79.35136	-124169.27	-140478.02	-119471.74	-72223.11	-109543.69	-128714.05	-109160.19
<i>Electronic Energy</i>	-1549.22639	-3294.80365	-4190.85096	-3059.37897	-3287.07702	-2456.50877	-418.56733	-3051.29876
<i>Core-Core Interaction</i>	2074071.14	4347810.53	6358802.94	4117684.77	4332741.05	3093118.70	6337014.58	4105.16073
<i>Heat of Formation</i>	607.96899	1182.86471	2316.08167	1184.01124	600.08990	1160.89629	2287.70695	1169.25586

4. CONCLUSIONS

In summary, the human hepcidin is the major regulatory hormone for iron homeostasis. In human urine, two predominant forms are comprised of 20 and 25 amino acids and only differing by N-terminal truncation. In this work, we investigated the behavior of Hepcidin-20 and Hepcidin- 25 in body and room temperatures, as well as the interaction human hepcidin peptides with carbon and boron nitride nanotubes. The influence of nanotubes on these two peptides is very interesting. Moreover, we presented the simulation of the interaction between the peptides and CNTs using the Monte Carlo and Semi-Empirical methods. According to the comparison trend in the methods of Semi-Empirical, the PM3 method presented results that are more acceptable rather than the AM1 method. During the simulation

using the Monte Carlo method, we observed that both peptides reached the equilibrium state of the potential energy after almost 35ns and its notable point is ΔE existing in the final state and initial state. ΔE value for the potential energy is reported for Hep20 and Hep25. This ΔE value shows fewer structure changes of Hep25 rather than Hep20 in the presence of nanotubes. By comparison of the available nanotubes (MWCNT, BNNT, and SWCNT), we reached to this result that created field by the SWCNT for both peptides has been caused more potential energy ΔE rather than other two nanotubes in two temperatures 300 K and 310 K. Finally, ΔE value for potential energy in 300°K is more negative than 310 K.

5. REFERENCES

- [1] Park C.H., Valore E.V., Waring A.J., Ganz T., Hepcidin, urinary antimicrobial peptide synthesized in the liver, *J. Biol. Chem*, 276, 7806–7810, **2001**.
- [2] Krause A., Neitz S., Magert H.J., Schulz A., Forssmann W.G., Schulz- Knappe, P., and Adermann, K. LEAP-1, a novel highly disulfide-bonded human peptide, exhibits antimicrobial activity, *FEBS Lett*, 480, 147–150, **2000**.
- [3] Pigeon C., Ilyin G., Courselaud B., Leroyer P., Turlin B., Brissot P., Lore´al O, A new mouse liver-specific gene, encoding a protein homologous to human antimicrobial peptide hepcidin, is overexpressed during iron overload, *J Biol Chem*, 276, 7811–7819, **2001**.
- [4] Peyssonnaux C., Zinkernagel A.S., Datta V., Lauth X., Johnson R. S. Nizet V, TLR4-dependent hepcidin expression by myeloid cells in response to bacterial pathogens, *Blood*, 107, 3727–3732, **2006**.
- [5] Howard N., Hunter D., Fulton B., Ganz T., Vogel H.J., The Solution Structure of Human Hepcidin, a Peptide Hormone with Antimicrobial Activity That Is Involved in Iron Uptake and Hereditary Hemochromatosis, *The Journal Of Biological Chemistry*, 277, 40, 37597–37603, **2002**.
- [6] Ganz T., Hepcidin, a key regulator of iron metabolism and mediator of anemia of inflammation, *Blood*, 102, 3, 783-788, **2003**.
- [7] Lombardi L., Maisetta G., Batoni G., Tavanti A., Insights into the Antimicrobial Properties of Hepcidins: Advantages and Drawbacks as Potential Therapeutic Agents, *Molecules*, 20, 6319-6341, **2015**.
- [8] Nemeth E., Tuttle M.S., Powelson J., Vaughn M.B., Donovan A., Ward D.M., Ganz T., Kaplan J., Hepcidin regulates cellular iron efflux by binding to ferroportin and inducing its internalization, *Science*, 306, 2090-2093, **2004**.
- [9] Kwapisz J., Slomka A., Zekanowska E., Hepcidin and its role in iron homeostasis, *J Int Fed Clin Chem*, 20, 2, 124–128, **2009**.
- [10] Hone J., Whitney M., Piskoti C., Zettl A., Thermal conductivity of singlewalled carbon nanotubes, *Physical Review B*, 59, 2514-2516, **1999**.
- [11] Tamsyn H.A., Hill J.M., Carbon nanotubes as drug delivery nanocapsules, *Curr. Appl. Phys.*, 8, 258-261, **2008**.
- [12] Krauss T.D., Biosensors: Nanotubes light up cells, *Nat Nanotechnol*, 4, 85–86, **2009**.
- [13] Hill J.M., Encapsulation of the Anticancer Drug Cisplatin into Nanotubes, *Nanoscience and Nanotechnology*, ICONN, 25–29, **2008**.
- [14] Hansen B.J., Liu Y., Yang R., Wang Z.L.. Hybrid Nanogenerator for Concurrently Harvesting Biomechanical and Biochemical Energy, *ACS nano*, 4, 3647–3652, **2010**.
- [15] Moradian R., Azadi S., Magnetism in defected single-walled boron nitride nanotubes, *Europhys. Lett.*, 83 ,17007-17011, **2008**.
- [16] Foldvari M., Bagonluri M., Carbon nanotubes as functional excipients for nanomedicines: I. Pharmaceutical properties, *Nanomedicine: NBM*, 4, 173-182, **2008**.
- [17] Blasé X., Rubio A., Louie S.G., Cohen M.L., Stability and band gap constancy of boron nitride nanotubes, *Europhys Lett.*, 28, 335, **1994**.
- [18] Ciofani G., Danti S., D’Alessandro D., Moscato S., Menciasci A., Assessing cytotoxicity of boron nitride nanotubes: Interference with the MTT assay, *Biochem Biophys Res Commun.*, 394, 2, 405–411, **2010**.
- [19] Nepal D., Balasubramanian S., Simonian A.L., Davis V.A., Strong antimicrobial coatings: single-walled carbon nanotubes armored with biopolymers, *Nano Lett.*, 8, 7, 1896–1901, **2008**.
- [20] Salvador-Morales C., Townsend P., Flahautc E., Vénien-Bryand C., Vlandase A., Greena M.L.H., Sim R.B., Binding of pulmonary surfactant proteins to carbon nanotubes; potential for damage to lung immune defense mechanisms, *Carbon*, 45, 607–617, **2007**.
- [21] Zuo G.H., Huang Q., Wei G.H., Zhou R.H., Fang H.P., Plugging into proteins: poisoning protein function by a hydrophobic nanoparticle, *ACS Nano*, 4, 7508–7514, **2010**.
- [22] Nel A.E., Mädler L., Velegol D., Xia T., Hoek E.M.V., Somasundaran P., Klaessig F., Castranova V., Thompson M., Understanding biophysicochemical interactions at the nano-bio interface, *Nat Mater*, 8, 543–557, **2009**.
- [23] Shim M., Kam N.W.S., Chen R.J., Li Y., Dai H., Functionalization of carbon nanotubes for biocompatibility and biomolecular recognition, *Nano Lett*, 2, 285–288, **2002**.
- [24] Xu Z., Zhang S., Weber J.K., Luan B., Zhou R., Li J., Sequential protein unfolding through a carbon nanotube pore, *Nanoscale* 8, 24, 12143–12151, **2016**.
- [25] Liu Z., Fan A.C., Rakhra K., Sherlock S., Goodwin A., Chen X., Yang Q., Felsher D.W., Dai H., Supramolecular Stacking of Doxorubicin on Carbon Nanotubes for in Vivo Cancer Therapy, *Angew. Chem., Int. Ed.*, 48, 7668–7672, **2009**.
- [26] Weng X., Wang M., Ge J., Yu S., Liu B., Zhong J., Kong J., Carbon Nanotubes as a Proteintoxin Transporter for Selective Her2- Positive Breast Cancer Cell Destruction, *Mol. BioSyst.*, 5, 1224– 1231, **2009**.
- [27] Chen X., Wu P., Rousseas M., Okawa D., Gartner Z., Zettl A., Bertozzi C.R., Boron nitride nanotubes are noncytotoxic and

can be functionalized for interaction with proteins and cells, *J. Am. Chem. Soc.*, 131, 890-891, **2009**.

[28] Cheng Y., Liu G.R., Li Z.R., Lu C., Mi D., Structure and magnetic properties of magnetron-sputtered FePt/Au superlattice films, *J. Phys. D: Appl. Phys.*, 41, **2008**.

[29] Becke A.D., Density-functional thermochemistry. III. The role of exact exchange, *J. Chem. Phys.*, 98, 5648–5652, **1993**.

[30] Lee, C., Yang, W., Parr, R.G. Development of the Colle-Salvetti correlation-energy formula into a functional of the electron density, *Phys. Rev. B*, 37, 785–789, **1988**.

[31] Bredow T., Jug K., Theory and range of modern semiempirical molecular orbital methods, *Theor Chem Acc*, 113, 1–14, **2005**.

[32] Moghaddam N.A., Ahmadi S., Rasoolzadeh R., Amino acid binding to nanotube: Simulation of membrane protein channels by computational methods, *Biosci. Biotech. Res. Comm.*, 9, 3, 495-502, **2016**.

[33] Zhao Q., Allostodynamic regulation of protein activity, *Quantum Matter*, 2, 9, **2013**.

[34] Kastner M., Communications in Nonlinear Science and Numerical Simulation, 15, 1589, 2010.

[35] HyperChem, Molecular Modelling System, Hypercube Inc., 1115 NW 4th Street, Gainesville, FL 32601, USA, **2009**.

[36] Jafari-Dehkordi S., Aghili Z., Ahmadi S., Jabbari S., Rezazadeh I., Hasani R., Rasoolzadeh R., Molecular Mechanics Investigation of Different Temperature Effects on *Bacillus licheniformis* α -amylase: A Computational Study, *Journal of pure and applied microbiology*, 9, 1, 607-611, **2015**.

[37] Roosta S., Nikkhar S.J., Sabzali M., Hashemianzadeh S.M., Molecular dynamics simulation study of boron nitride nanotubes as

a drug carrier: from encapsulation to releasing, *RSC Adv*, 6, 9344–9351, **2016**.

[38] Ghaheh H.S., Mousavi M., Araghi M., Rasoolzadeh R., Hosseini Z., Nanobiological studies on drug design using molecular mechanic method, *Advanced Biomedical Research*, 4, 219, **2015**.

[39] Yahyaei H., Monajjemi M., Theoretical Study of Different Solvent and Temperature Effects on Doublewalled Carbon Nanotubes (DWNTs) and Calixarene with Amino Acid: A QM/MM Study, *Fullerenes, Nanotubes and Carbon Nanostructures*, 22, 346–361, **2014**.

[40] Najafabadi A.S., Ahmadi S., Fardin M.M., Rasoolzadeh R., Vajedi F., Molecular Simulation of GABA(A) Receptor to Study of Effects on Nervous Stimulants Inhibitory & Blood Pressure; A Nano Molecular Modeling of GABARAP, *Biosciences biotechnology research Asia*, 12, 1, 419-424, **2015**.

[41] Mollaamin F., Monajjemi M., Harmonic Linear Combination and Normal Mode Analysis of Semiconductor Nanotubes Vibrations, *Journal of Computational and Theoretical Nanoscience*, 12, 1030–1039, **2015**.

[42] Yahyaei H., Monajjemi M., Aghaie H., Zare K., Monte Carlo Quantum Calculation for Double-Walled Carbon Nanotubes (DWNTs) Combined to Calixarene[6], *Journal of Computational and Theoretical Nanoscience*, 10, 2332–2341, **2013**.

[43] Salehi R., Rasoolzadeh R., Investigation of Capecitabine and 5-fluorouracil anticancer drugs structural properties and their interactions with single-walled carbon nanotube: insights from computational methods, *Biointerface Research in Applied Chemistry*, 8(1), 3075 – 3083, **2018**.

6. ACKNOWLEDGEMENTS

The authors would like to thank Fahimeh Sadat Vajedi, Samira Jahangiri for their assistance.

© 2018 by the authors. This article is an open access article distributed under the terms and conditions of the Creative Commons Attribution license (<http://creativecommons.org/licenses/by/4.0/>).